Submitted to Astrophysical Journal

HST Observations of New Horizontal Branch Structures in the Globular Cluster ω Centauri[1]

Noella L. D'Cruz[2], Robert W. O'Connell, Robert T. Rood, Jonathan H. Whitney, Ben Dorman[3]
Department of Astronomy, University of Virginia, P.O.Box 3818, Charlottesville VA 22903; noella@physics.usyd.edu.au, rwo@virginia.edu, rtr@virginia.edu, jw9w@virginia.edu, bd4r@virginia.edu

Wayne B. Landsman, Robert S. Hill
Laboratory for Astronomy & Solar Physics, Code 681/ Raytheon STX, NASA Goddard Space Flight Center, Greenbelt MD 20771; landsman@mpb.gsfc.nasa.gov, bhill@uit.gsfc.nasa.gov

Theodore P. Stecher
Laboratory for Astronomy & Solar Physics, Code 681, NASA Goddard Space Flight Center, Greenbelt, MD 20771; stecher@uit.gsfc.nasa.gov

Ralph C. Bohlin
Space Telescope Science Institute, Baltimore, MD 21218; bohlin@fos.stsci.edu

ABSTRACT

The globular cluster ω Centauri contains the largest known population of very hot horizontal branch (HB) stars. We have used the Hubble Space Telescope to obtain a far-UV/optical color-magnitude diagram of three fields in ω Cen. We find that over 30% of the HB objects are "extreme" HB or hot post-HB stars. The hot HB stars are not concentrated toward the cluster center, which argues

[1] Based on observations with the NASA/ESA Hubble Space Telescope, obtained at the Space Telescope Science Institute, which is operated by the Association of Universities for Research in Astronomy, Inc. under NASA contract No. NAS5-26555.

[2]Current Address: Chatterton Astronomy Department & Research Centre for Theoretical Astrophysics, A-28 School of Physics, University of Sydney, NSW 2006, Australia

[3]Current Address: Raytheon ITSS, Code 644, NASA/GSFC, Greenbelt MD 20771; dorman@veris.gsfc.nasa.gov

against a dynamical origin for them. A wide gap in the color distribution of the hot HB stars appears to correspond to gaps found earlier in several other clusters. This suggests a common mechanism, probably related to giant branch mass loss. The diagram contains a significant population of hot sub-HB stars, which we interpret as the "blue-hook" objects predicted by D'Cruz et al. (1996a). These are produced by late He-flashes in stars which have undergone unusually large giant branch mass loss. ω Cen has a well-known spread of metal abundance, and our observations are consistent with a giant branch mass loss efficiency which increases with metallicity.

Subject headings: globular clusters: individual (ω Cen)—stars: evolution—stars: horizontal branch—stars: mass loss—stars: Population II—ultraviolet: stars

1. Introduction

Globular clusters contain the largest samples of old stellar populations appropriate for studying late stages of stellar evolution, especially the horizontal branch. This consists of core helium-burning, shell hydrogen-burning stars, with cores of approximately the same mass but envelopes of a range of mass (Iben & Rood 1970). For a given composition, envelope mass determines horizontal branch (HB) temperature, with smaller envelopes yielding higher temperatures. The variation in envelope mass is due to dispersion in mass loss during the preceding red giant branch (RGB) phase. However, the RGB mass loss process and the physical quantities on which it depends are poorly understood.

Only with the advent of space-based imaging with the Hubble Space Telescope (HST) and the *Astro*/Ultraviolet Imaging Telescope (UIT, Stecher 1997) has it become feasible to study large samples of the hottest (and lowest envelope mass) HB stars. These objects are brightest in the vacuum-UV band accessible to space telescopes. But equally important, globular cluster cores, which are impossible to study from the ground because of image-crowding from cool stars, can be studied from space because the cool stars are either suppressed in the UV or resolved by the high spatial resolution in the visible with HST. Complete samples of hot stars can therefore be obtained.

The hot HB populations of a number of globular clusters have recently been studied, including ω Centauri, M3, M13, M79, M80, NGC 362, NGC 2808, NGC 6388, NGC 6441, and NGC 6752 (e.g. Whitney et al. 1994; Moehler, Heber & de Boer 1995; Hill et al. 1996; Landsman et al. 1996; Ferraro et al. 1997; Sosin et al. 1997; Rich et al. 1997; Dorman et al. 1997; O'Connell et al. 1997; Catelan et al. 1998; Ferraro et al. 1998). This work has revealed

several important features of the hot horizontal branch. *(i)* Some HBs extend nearly all the way to the He-burning main sequence, having temperatures $\gtrsim 16000\,\mathrm{K}$ and envelope masses of $\lesssim 0.05 M_{\odot}$, presumably due to extreme RGB mass loss rates. This region is called the "extreme horizontal branch" (EHB). *(ii)* Some clusters have significant populations of hot stars lying above the HB. These are probably post-EHB objects which, because of their small envelopes never reach the thermally pulsing stage on the asymptotic giant branch (AGB) and instead spend most of their post-HB lifetime at high temperatures. EHB descendents evolve along either post-early AGB tracks or "AGB-manqué" tracks (e.g. Greggio & Renzini 1990). *(iii)* Some HBs have significantly underpopulated regions or "gaps," and these can occur at similar temperatures in different clusters (Ferraro et al. 1998). *(iv)* In the case of ω Cen, there appear to be hot stars lying below the HB (Whitney et al. 1994). All of these features are probably related to physical processes on the RGB that determine the distribution of HB envelope masses.

In this paper, we discuss new far-UV/visible HST observations of the globular cluster ω Centauri, which is an important benchmark system in several ways. It exhibits a spread in metallicity: $-2.2 \lesssim [\mathrm{Fe/H}] \lesssim -0.8$ (Norris, Freeman, Mighell 1996, Greenlaw 1993, Woolley 1966), which makes it a better analogue to the old populations of external galaxies than most local clusters. (Evidence for multiple generations of star formation suggest that ω Cen itself may even be a captured galaxy nucleus, Hughes & Wallerstein 1999.) Its HB is extremely blue, and it contains the largest identified population of EHB and of putative EHB-descendent stars lying above the HB (Dickens et al. 1988, Bailyn et al. 1992, Whitney et al. 1994). We are particularly interested in investigating the reality of two unusual HB features found in lower-precision far-UV photometry by the UIT: a hot HB gap and sub-HB stars (Whitney et al. 1994).

2. Observations and Data Reduction

We have used HST to observe ω Cen in the far-UV and visual bands as part of GO program 6053. The images discussed here are Wide Field Planetary Camera 2 (WFPC2) "acquisition frames" taken to confirm astrometry for a set of spectroscopic targets (to be discussed elsewhere) identified on UIT far-UV images by Whitney et al. (1994). Compared to the Whitney et al. study, the HST data has smaller photometric errors, better astrometry, and an optical comparison image better matched to the UV. Three fields in ω Cen were observed with WFPC2 in the F160W and F555W filters. Total exposure times for each field were 1400 secs in F160W and 8 sec in F555W, each split into two parts to allow the elimination of most cosmic ray events via a simple combination program. The fields

were located 1.′34, 2.′62, and 4.′57 from the cluster center (R.A. = $13^{\mathrm{h}}\,26^{\mathrm{m}}\,45\overset{\mathrm{s}}{.}9$; DEC = $-47^\circ\,28'\,37''$, J2000). The choice of the three fields is based on the position of stars for which UV spectra were obtained.

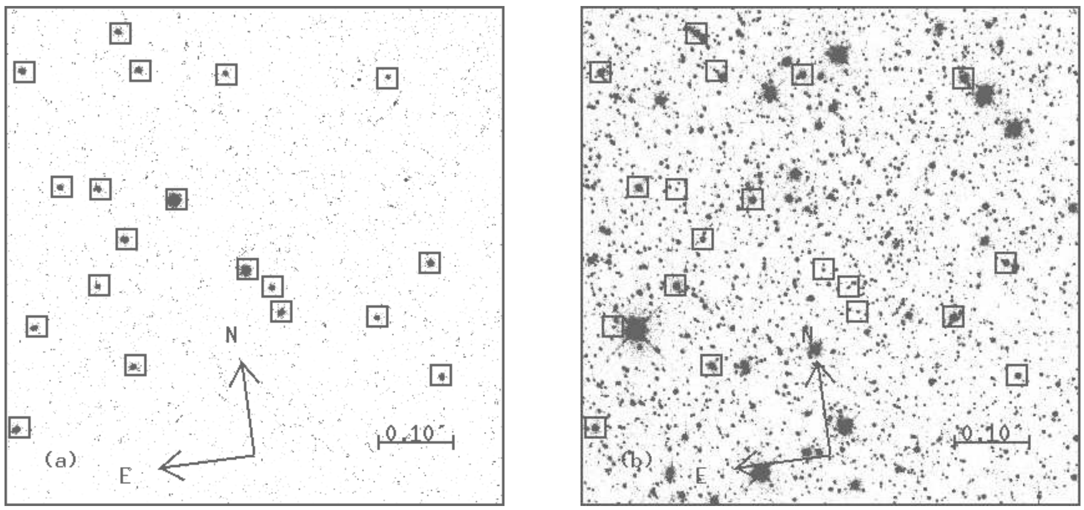

Fig. 1.— (a) Far-UV and (b) V frames of part of our HST/WFPC2 field at a radius of 2.′62 from the center of ω Cen. UV sources and their visual counterparts are marked. The boxes are centered on the V band centroids, and the offsets between the stars and the V-centroids in (a) shows the extent of geometric distortion.

Figure 1 compares the far-UV and V images of part of one of our fields. There are about 100 times as many sources present on the F555W frame as on the F160W frame. F555W counterparts could be identified for most of the F160W sources in the field if the geometric distortion in the far-UV filter is taken into account (Biretta 1996). The identifications are marked on both frames in Fig. 1 with the boxes centered on the V band centroids. The offsets between the box centers and the star images on the far-UV frame illustrate the extent of the image distortion. A brief inspection of the UV frames indicates that there is vignetting in the filter and that the images are affected by coma, but there are no blended images. Aperture photometry was carried out on the UV sources using an IDL implementation of DAOPHOT (Stetson 1987). The area around each star was cleaned to make sure that no cosmic rays or nearby stars contaminated the sky magnitude. Contamination effects on our UV images (Holtzman et al. 1995) were minimal since our observations were taken only one day after a decontamination cycle.

Obtaining stellar magnitudes from the V band frames required point spread function (PSF) fitting, for which we used the FORTRAN version of DAOPHOT II (Stetson 1992).

Aperture corrections were assumed to be constant with magnitude for the recommended aperture of $1''$ in diameter (Holtzman et al. 1995). Results were converted into the STMAG magnitude system as described by Holtzman et al. For a monochromatic flux, F_λ (in units of $\mathrm{erg\,s^{-1}\,cm^{-2}\,\AA^{-1}}$) , at a wavelength λ, STMAG $= -2.5 \times \log F_\lambda - 21.1$.

3. Results and Discussion

3.1. *The UV-Optical CMD*

Figure 2 shows the resulting $m(160), (160 - V)$ color-magnitude diagram for the three fields combined. There are 406 stars in the CMD from a total of 473 UV sources in the three fields. Of the 67 sources that do not appear in the CMD, 3 are on bad columns in the UV, 21 are either near the edge of the chip or too close to another star to measure in the UV, 8 have no V counterpart (these may not be stellar), and 35 (mostly in the more crowded central region) are too faint to measure accurately in V. Many of these 35 could be EHB and AGB-manqué stars since they are relatively bright in the UV. The detection limit is the dot-dashed line on the figure.

Two zero-age HBs (ZAHBs) have been plotted on the observed color magnitude diagram, corrected for ω Cen's distance modulus of 13.57 (Dickens, et al. 1988) and interstellar reddening of $E(B-V) = 0.15$ taken from Whitney et al. (1994) and Greenlaw (1993). These values produce the best overall match between the theoretical and observed sequences. We use the UV extinction law of Cardelli, Clayton & Mathis (1989). The upper solid line is the ZAHB for [Fe/H] $= -2.2$ while the lower line is for [Fe/H] $= -1.5$. Typical errors in the data are shown on the right side of Figure 2.

The main features of interest in the CMD in Fig. 2 are the following:

1. The cooler HB stars with $-0.5 \lesssim (160 - V) \lesssim 2.0$ ($T_{\rm eff} \sim 8000$ to $11000\,$K) fit the predicted locus of the ZAHB well, with only a small difference in mean slope (the data being slightly flatter than the models). They show relatively little vertical scatter. By contrast, the hotter objects at comparable $m(160)$ magnitudes show large scatter, which must therefore be cosmic, not photometric errors.

2. The approximate position of the cool end of the heavily populated segment of the blue HB is marked on the CMD. The limiting magnitude of the UV images is significantly fainter than this, so the reduced population is not a detection artifact. The boundary lies at $T_{\rm eff} \sim 7600\,$K, based on the Dorman models. Stars redder than this tend to lie

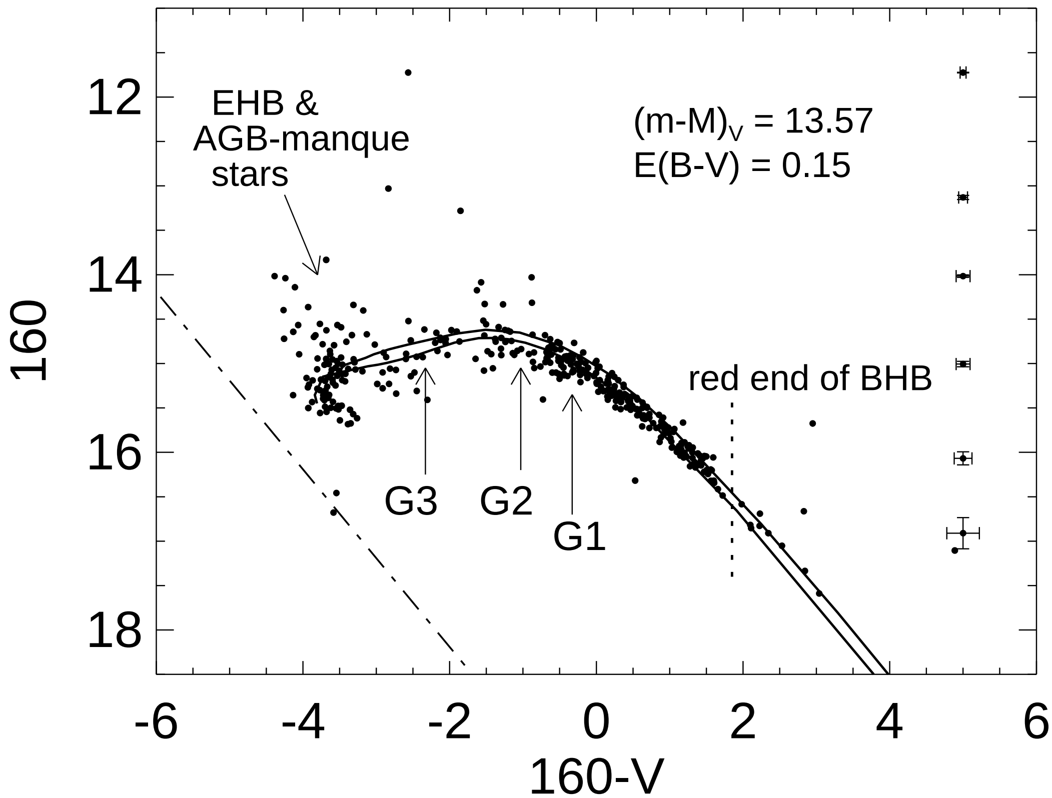

Fig. 2.— The observed $m(160), (160-V)$ color-magnitude diagram for 406 stars in ω Centauri. The upper solid line is a ZAHB for [Fe/H] $= -2.2$, while the lower line is for [Fe/H] $= -1.5$ from Dorman (1997), transformed using the distance modulus and extinction given in the figure. The upper detection limit is shown by the dot-dashed line. Typical photometric error bars are shown at the right. There is a large sub-HB population most conspicuous at the hot end of the HB but extending several magnitudes in $(160-V)$. A number of AGB-manqué or other post-HB stars are seen above the HB. The approximate position of the red end of the BHB is marked. The locations of the HB gaps, G1, G2, G3, found by Ferraro et al. (1998) in M13 and M80, are shown.

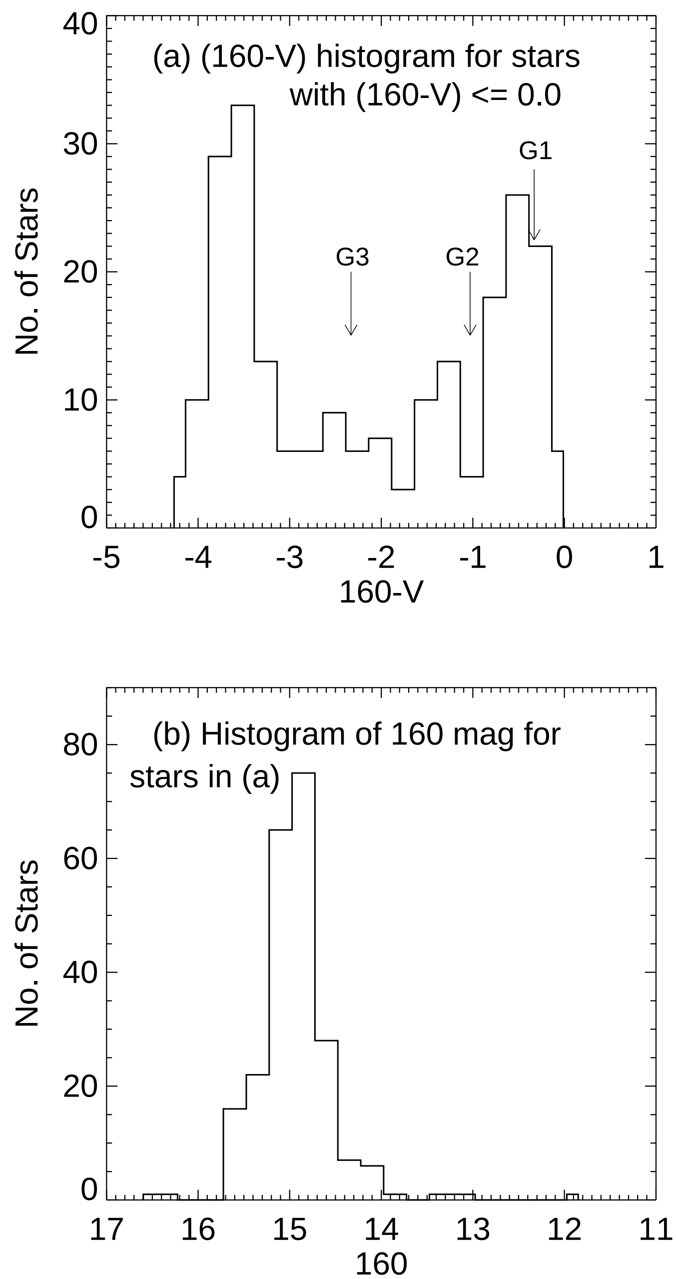

Fig. 3.— (a) Histogram of $(160 - V)$ colors for stars on the "horizontal" part of the hot HB in ω Cen bluer than $(160 - V) = 0.0$. The locations of HB gaps, G1, G2, G3, found by Ferraro et al. (1998) in M13 and M80, are shown. (b) Histogram of $m(160)$ magnitudes for the stars in (a), showing the presence of both post-HB evolved stars (brighter than the HB) and sub-HB stars.

above the HB and are probably evolved BHB stars rather than ZAHB stars.

3. About 32% of the HB sample is composed of EHB stars, with $(160 - V) \lesssim -1.9$. The objects lying more than 0.2 mag above the predicted EHB are probably AGB-manqué descendents of EHB stars. A total of 389 such objects were found in the larger field sampled by UIT.

4. There is a large sparsely populated region in the HB from $-3.0 \lesssim (160 - V) \lesssim -0.5$ ($22500\,\mathrm{K} \lesssim T_{\mathrm{eff}} \lesssim 11000\,\mathrm{K}$). This is shown more clearly in Figure 3(a) which plots the $(160 - V)$ distribution for stars with $(160 - V) \leq 0$ (where the HB is approximately horizontal). This underpopulated region corresponds to the part of the HB where Ferraro et al. (1998) found gaps in M13, M80 and M3. We have marked the approximate position of the gaps G1, G2, and G3 from Figure 4 of Ferraro et al. in both Figs. 2 and 3(a) after correcting for the reddening difference between the clusters. It appears that there is a broad gap in ω Cen corresponding to G3 and a narrower one corresponding to G2 (though the statistics are not good) but that G1 is clearly absent.

5. The HST observations confirm, with good photometric precision, the presence of sub-HB stars, as found by UIT. A histogram of $m(160)$ magnitudes for the hot HB is shown in Figure 3(b). The mode of the blue HB occurs at $m(160) = 15.2$, and the expected post-HB objects lie at brighter magnitudes. However, there is a tail of fainter objects up to 0.7 mags fainter. Most are concentrated near the hot end of the EHB; however, other sub-HB objects are found at colors as red as $(160 - V) \sim -0.5$.

3.2. *Spatial Distribution of Hot Stars*

There is no evidence from their spatial distribution that the EHB objects in ω Cen are binary stars or that dynamical effects are important in their production. Binaries or the products of strong interactions in the cluster core would tend to be more concentrated to the cluster center. Instead, in the large-field ($40'$ diameter) UIT images of (Whitney et al. 1994), the radial distribution of ω Cen's EHB stars follows that of the rest of the HB stars. Our HST data suggest that the fraction of EHB stars increases outwards from about $28 - 33\%$ in the inner two fields to about 43% in the outer field. This relatively modest effect is possibly an artifact of our inability to obtain V-band magnitudes for the fainter hot objects in the cluster's interior.

3.3. *Horizontal Branch Gaps*

It is likely that the HB gaps apparent in Figs. 2 and 3(a) are connected to the distribution of envelope masses produced by the RGB mass loss process. Rood, Whitney & D'Cruz (1997) have shown that HB gaps cannot arise from post-ZAHB evolution if the distribution of envelope masses is uniform.

Whitney et al. (1998) modeled the broad G3 gap which was detectable in the earlier UIT data using smooth distributions in total ZAHB mass or in the mass loss efficiency parameter η (from Reimers' mass loss formula, Reimers 1977). They incorporated the models of D'Cruz et al. (1996a), in which the effects of mass loss (as specified by η) on RGB evolution are followed in detail and the "blue hook" population is included. They found that a flat distribution in η, when combined with the known distribution of metallicity, best reproduced the broad G3 gap and the sub-HB stars in the UIT data. The metallicity spread would presumably act to blur finer structure in the ω Cen HB, whatever the mechanism for its origin.

Ferraro et al. (1998) suggest that gaps are located at roughly the same effective temperatures in different clusters, though not all clusters have the same number of gaps. The hottest gap, G3, is found in extreme "blue tail" clusters (Fusi Pecci et al. 1993), and may indicate the onset of EHB behavior. The ω Cen HB extends further to the blue than the HBs of M13 and M80. This could imply that mass loss efficiency is greater in ω Cen than in M13 and M80. The Whitney et al. model does not explain the presence of multiple gaps, which suggest the existence of several mass loss mechanisms operating with different efficiencies in different clusters. Sweigart's (1997) models which involve rotationally-induced envelope mixing of He on the RGB, predict larger amounts of mass loss due to increased luminosity of the red giant tip. It is possible that the onset of increased mixing could manifest itself on the HB as a gap.

3.4. *Sub-HB Stars and Metallicity Dependence of Mass Loss*

ω Cen is the only cluster in which there is now clear evidence for sub-HB objects. Whitney et al. (1998) interpreted the sub-HB objects in the UIT sample as the "blue hook" stars predicted in the models of D'Cruz et al. (1996a). These are objects which, due to extreme amounts of RGB mass loss, left the RGB before the He flash but were able to ignite He later as they started moving down the high temperature part of the white dwarf sequence. They are predicted to lie at the very blue end of the ZAHB. Their core masses could be as much as $0.015\,M_{\odot}$ below canonical values, which will cause them to lie up to 0.1 mag below the ZAHB. The computations of Sweigart (1999) suggest that the blue hook stars might

have higher temperatures ($\log T_{\rm eff} \sim 4.6$) than typical EHB stars, and surface abundances enriched in helium and carbon. At these high temperatures, even the $(160-V)$ colors do not provide good $T_{\rm eff}$ discrimination, so that followup spectroscopy would be useful to provide constraints on both the temperatures and the abundances.

Some of the sub-HB stars are also likely to be affected by radiative levitation. The lowest temperature at which they appear in the CMD is $T_e \sim 11,000$ K, roughly the temperature expected for the onset of radiative levitation of iron, which would cause them to be up to another 0.1 mag fainter in $m(160)$ (Grundahl et al. 1999, Behr et al. 1999, Moehler et al. 1999).

However, the stars in Fig. 2 lie farther below the ZAHB than predicted by the models. The metallicity spread in ω Cen may account for some of the differences between the observed and predicted CMDs. Metal poor HB stars are more luminous than metal rich HB stars of the same $T_{\rm eff}$. The observed CMD would be more consistent with the models if the metallicity of the HB stars *increases* with increasing effective temperature. This would produce the flatter slope for the observed CMD than for a single metallicity theoretical ZAHB, just as observed for $(160 - V) \gtrsim -1$. In this interpretation, the sub-HB stars would mostly be metal rich blue hook stars.

If, indeed, metallicity increases with effective temperature along the cluster's HB, then this suggests that mass loss efficiency increases with metallicity. This result is consistent with the determination of [Ca/H] in the cluster's cooler BHB stars, where a large fraction of the cooler BHB stars with $7500\,{\rm K} \lesssim T_{\rm eff} \lesssim 8200\,{\rm K}$ are found to be metal poor ($\langle[{\rm Fe/H}]\rangle = -1.95$) (D'Cruz et al. 1996b; D'Cruz 1998). The calcium abundance distribution of the giants and RR Lyraes is peaked at the higher metallicity of $[{\rm Fe/H}] = -1.7$, possibly indicating that HB stars of this metallicity or higher dominate the abundance distribution at higher temperatures.

Finally, we note that a mass loss efficiency which increases with metallicity, as suggested by our data, is in the correct sense to explain the well-known correlation between far-UV output and metal abundance in elliptical galaxies (Burstein et al. 1988, Greggio & Renzini 1990; Dorman, O'Connell, & Rood 1995; Yi, Demarque, & Oemler 1997).

4. Conclusion

HST observations of ω Cen confirm the substantial population of sub-HB, EHB, and AGB-manqué stars found by Whitney et al. (1994) with UIT. About 32% of the HB consists of EHB stars and their descendents. The density of EHB objects relative to the total HB

does not decrease with radius, contrary to expectations if they are in binary systems or if dynamical interactions in the cluster core are critical for their production. The sub-HB stars are probably "blue-hook" stars produced by RGB stars with large mass loss which experience He ignition after leaving the RGB. A broad gap in the blue HB seen in earlier work is confirmed and corresponds to two of the hotter gaps found in the clusters M13 and M80, possibly blurred by ω Cen's metallicity spread. The gaps probably contain information on RGB mass loss mechanisms.

Comparison of the observed CMD to theoretical ZAHB models suggests that RGB mass loss efficiency may increase with metallicity and that the sub-HB stars are the most metal-rich. This is in the correct sense to explain the well-known correlation between far-UV output and metal abundance in elliptical galaxies.

Acknowledgements: We are grateful to Barbara Paltrinieri, Francesco Ferraro, and Jamie Ostheimer for their help with the data reduction. This research was supported in part by STScI grant GO-06053 and NASA grants NAG5-700 and NAG5-6403.

REFERENCES

Bailyn, C., Sarajedini, A., Cohn, H., Lugger, P. M., & Grindlay, J. E. 1992, AJ, 103, 1564

Behr, B. B., Cohen, J. G., McCarthy, J. K., & Djorgovski, S. G., 1999, ApJ, 517, L135

Biretta, J. 1996 ed. WFPC2 Instrument Handbook, version 4.0.

Burstein, D., Bertola, F., Buson, L. M., Faber, S. M. & Lauer, T. 1988, ApJ, 328, 440

Cardelli, J. A., Clayton, G. C., & Mathis, J. S. 1989, ApJ, 345, 245

Catelan, M., Borissova, J., Sweigart, A. V., & Spassova, N. 1998, ApJ, 494, 265

D'Cruz, N. L. 1998, Ph.D. thesis, University of Virginia

D'Cruz, N. L., Dorman, B., Rood, R. T., & O'Connell, R. W. 1996a, ApJ, 466, 359

D'Cruz, N. L., Dickens, R. J., Hatzidimitriou, D., Rood, R. T., & O'Connell, R. W. 1996b, in Advances in Stellar Evolution, ed. by R. T. Rood and A. Renzini, (Cambridge: CUP), 100

Dickens, R. J., Brodie, I. R., Bingham, E. A., & Caldwell, S. P. 1988, in R.A.L. Report no. 88-04

Dorman, B. 1997, private communication

Dorman, B., O'Connell, R. W., & Rood, R. T. 1995, ApJ, 442, 105

Dorman, B., Shah, R. Y., O'Connell, R. W., Landsman, W. B., Rood, R. T., Bohlin, R. C., Neff, S. G., Roberts, M. S., Smith, A. M., & Stecher, T. P. 1997, ApJ, 480, L31

Ferraro, F. R., Paltrinieri, B., Fusi Pecci, F., Cacciari, C., Dorman, B., & Rood, R. T. 1997, ApJ, 484, L145

Ferraro, F. R., Paltrinieri, B., Fusi Pecci, F., Dorman, B., & Rood, R. T. 1998, ApJ, 500, 311

Fusi Pecci, Ferraro, F. R., Bellazzini, M., Djorgovski, S. G., Piotto, G., & Buonanno, R. 1993, AJ, 105, 1145

Greenlaw, R. B. L. 1993, Ph.D. thesis, University of Leeds

Greggio, L. & Renzini, A. 1990, ApJ, 364, 35

Grundahl, F., Catelan, M., Landsman, W. B., Stetson, P. B., & Andersen, M. I., 1999, submitted to ApJ (astro-ph/9903120)

Hill, R. S., Cheng, K. P., Smith, E. P., Hintzen, P. M. N., Bohlin, R., & O'Connell, R. W. 1996, AJ, 112, 2909

Holtzman, et al. 1995, PASP, 107, 1065

Hughes, J., & Wallerstein, G. 1999, AJ, in press

Iben, I., Jr., & Rood, R. T. 1970, ApJ, 161, 587

Landsman, W. B., Sweigart, A. V., Bohlin, R. C., Neff, S. G., O'Connell, R. W., Roberts, M. S., Smith, Andrew M. & Stecher, T. P. 1996 ApJ, 472, L93

Moehler, S., Heber, U., & de Boer, K. S. 1995 A&A, 294, 65

Moehler, S., Sweigart, A. V., Landsman, W. B., Heber, U., & Catelan, M. 1999 A&A, 346, L1

Norris, J. E., Freeman, K. C. & Mighell, K. J. 1996, ApJ, 462, 241

O'Connell, R. W., Dorman, B., Shah, R. Y., Rood, R. T., Landsman, W. B., Witt, A. N., Bohlin, R. C., Neff, S. G., Roberts, M. S., Smith, A. M., & Stecher, T. P. 1997, AJ, 114, 1982

Reimers, D. 1977, A & A, 57, 395

Rich, R. M, Sosin, C., Djorgovski, S. G., Piotto, G., King, I. R., Renzini, A., Phinney, E. S., Dorman, B., Liebert, J., & Meylan, G. 1997, ApJ, 484, L25

Rood, R. T., Whitney, J. H., & D'Cruz, N. L. 1997 in Advances in Stellar Evolution, ed. R. T. Rood & A. Renzini, (Cambridge: CUP), 74

Sosin, C., Dorman, B., Djorgovski, S. G, Piotto, G., Rich, R. M., King, I. R., Liebert, J., Phinney, E. S., & Renzini, A. 1997, ApJ, 480, L35

Stecher, T. P. et al. 1997, PASP, 109, 584

Stetson, P. B. 1992, Astronomical Data Analysis Software and Systems I, A.S.P. Conference Series, Vol. 25, eds. D. M. Worrall, C. Biemesderfer, and J. Barnes (San Francisco:ASP), 297.

Stetson, P. B. 1987, PASP, 99, 191

Sweigart, A. V. 1997, ApJ, 474, L23

Sweigart, A. V. 1999, in The Third Conference on Faint Blue Stars, ed. A. G. D. Philip, J. Liebert, & R. A. Saffer (Cambridge: Cambridge Univ. Press), 3

Whitney, J. H., et al. 1994, AJ, 108, 1350

Whitney, J. H., et al. 1998, ApJ, 495, 284

Woolley, R. v. d. R. 1966, Royal Obs. Annals, 2

Yi, S., Demarque, P., & Oemler, A., Jr. 1998, ApJ, 492, 480

This preprint was prepared with the AAS LaTeX macros v4.0.